

## Theory of oscillations in average crisis-induced transient lifetimes

Krzysztof Kacperski\* and Janusz A. Hołyst†

Max Planck Institute for Physics of Complex Systems, Nöthnitzer Straße 38, 01187 Dresden, Germany  
and Institute of Physics, Warsaw University of Technology, Koszykowa 75, PL-00-662 Warsaw, Poland  
(Received 16 November 1998)

Analytical and numerical study of the roughly periodic oscillations emerging on the background of the well-known power law governing the scaling of the average lifetimes of crisis induced chaotic transients is presented. The explicit formula giving the amplitude of “normal” oscillations in terms of the eigenvalues of unstable orbits involved in the crisis is obtained using a simple geometrical model. We also discuss the commonly encountered situation when normal oscillations appear together with “anomalous” ones caused by the fractal structure of basins of attraction. [S1063-651X(99)02407-1]

PACS number(s): 05.45.Ac

### I. INTRODUCTION

Crises [1] appearing in nonlinear dissipative systems exhibiting deterministic chaos are abrupt changes undergone by a chaotic attractor due to its collision with an unstable periodic orbit  $B$ , when a system parameter  $p$ , varied continuously, crosses a critical value  $p_c$ . The phenomenon can also be described as the collision of the stable manifold  $w_s^{(B)}$  of  $B$  with the unstable manifold  $w_u^{(A)}$  of another orbit  $A$  of the same period embedded in the attractor (heteroclinic crisis) or the unstable manifold  $w_u^{(B)}$  of  $B$  itself (homoclinic crisis). One of the branches of the stable manifold  $w_s^{(B)}$  is the boundary of basin of the attractor, which is in turn the closure of one of the branches of the unstable manifold  $w_u$ .

In the dynamics after crisis (for  $p \gtrsim p_c$ ) characteristic transients appear [2]; the system remains for some time on the former (precritical) attractor, which is now a chaotic saddle. In the case of a *boundary crisis* the transient is followed by a definitive escape to some other attractor in the phase space, while after an *interior crisis* transients are interrupted by (typically short) bursts to an extension of the precritical attractor. After an *attractor merging crisis* we have intermittent jumps between symmetric precritical parts of the attractor.

For a large class of dynamical systems the time  $t$  that the system stays on the precrisis attractor has an exponential probability distribution  $Pr(t) = (1/T)\exp(-t/T)$  with a mean value  $T$  obeying a power scaling law [2]

$$T \sim (p - p_c)^{-\gamma}. \quad (1)$$

For most two-dimensional dissipative maps, the exponent  $\gamma > 0$  can be expressed in terms of the eigenvalues  $\lambda_1$  ( $|\lambda_1| > 1$ ) and  $\lambda_2$  ( $|\lambda_2| < 1$ ) of the saddle orbit  $A$  for heteroclinic crisis [2,3]:

$$\gamma = \frac{1}{2} + \frac{\log|\lambda_1|}{|\log|\lambda_2||}, \quad (2)$$

or of the orbit  $B$  for homoclinic crisis:

$$\gamma = \frac{\log|\lambda_2|}{2 \log|\lambda_1\lambda_2|}. \quad (3)$$

The power law (1) and the formulas (2) and (3) have been confirmed in many numerical and experimental studies (e.g., [4–6]).

However, it has also been noticed [7,3] that Eq. (1) describes only the general tendency of the function  $T(p - p_c)$ , and imposed on it one can observe some oscillations (cf. Figs. 3 and 4) resulting from a ragged (fractal) measure of the chaotic attractor colliding with its basin of attraction [8]. In the case of a homoclinic crisis their period on a log-log plot of  $T(p - p_c)$  is  $|\log|\lambda_2||$ , and their amplitude is large for small  $|\lambda_2|$ . These oscillations have been indicated as a potential complication to verifying the scaling law (1) and determining the critical exponent  $\gamma$ . Further on we shall refer to these attractor induced oscillations as *normal oscillations*.

Recently [9] we studied another kind of oscillation caused by the intertwined (typically fractal) structure of precritical basins of attraction [10,11]. We called them *anomalous*, because of the appearance of increasing pieces of the function  $T(p - p_c)$ , contrary to the general decreasing trend (1). The maximal amplitude of the oscillations has been calculated using a simple model of a self-similar intertwined basin. Oscillations of both kinds can be noticed on  $T(p - p_c)$  plots obtained for crises in different systems studied numerically [12] and experimentally [5].

In this paper we derive a formula for the amplitude of the attractor-induced oscillations in systems that can be reduced to two dimensional maps for the generic case when the tangency of manifolds at the crisis point is quadratic (Sec. II). In Sec. III the typical case when both kinds of oscillation appear together is discussed.

### II. ATTRACTOR-INDUCED OSCILLATIONS

As a consequence of crisis the chaotic attractor becomes a chaotic saddle, and almost every point, after a transient of average length  $T$ , finally diverges from it. However, for  $p \gtrsim p_c$  we can define a *pseudobasin* as a set of initial conditions evolving to the saddle after, say,  $M$  iterations, where

\*Electronic address: kacper@if.pw.edu.pl

†Electronic address: jholyst@if.pw.edu.pl

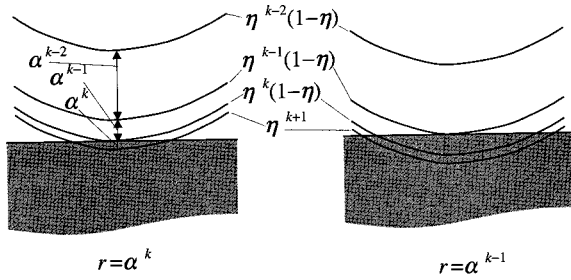


FIG. 1. Model attractor  $\mathcal{Q}_n$  for  $n = k + 1$  penetrating the basin of escape at  $r = \alpha^k$  and  $r = \alpha^{k-1}$ .

$M \ll T$ . The structure of the pseudobasin is very similar to that of the real basin before crisis. In what follows, we shall refer to the complement of the postcritical pseudobasin as the basin of escape, for the trajectory leaves the chaotic saddle soon after entering it.

The average transient time  $T$  is proportional to the inverse of the measure  $\mu$  of the part of the saddle overlapping the basin of escape [2],

$$T(p-p_c) \sim \frac{1}{\mu(p-p_c)}. \quad (4)$$

### A. The model of the chaotic saddle

In order to assess the amplitude of normal oscillations we introduce a model of the fragment of the chaotic attractor (which becomes a chaotic saddle at the crisis point) colliding with the boundary of its basin of attraction. Assume that the half-plane  $y < 0$  is the (nonfractal) basin of escape. Imagine, as the first approximation, that the chaotic saddle in the vicinity of the tangency point consists of two parabolic segments:  $A_1^{(1)} = \{(x, y) : y = x^2 + a - r\}$  and  $A_2^{(1)} = \{(x, y) : y = x^2 - r\}$ . The measure  $\mu$  of the considered fragment is distributed uniformly along both segments, its  $\eta$  part falling on  $A_2^{(1)}$  and the remaining  $1 - \eta$  on  $A_1^{(1)}$ ,  $\eta \in (0, 1)$ . The quantity  $r \sim p - p_c$  corresponds to the bifurcation parameter of the system measured as the distance from the crisis point. In the second step we assume that the segment:  $A_2^{(1)}$  is composed of two subsegments:  $A_2^{(2)} = \{(x, y) : y = x^2 + \alpha a - r\}$  and  $A_3^{(2)} = \{(x, y) : y = x^2 - r\}$ ,  $\alpha \in (0, 1)$ , with the measure distribution  $\mu(A_2^{(2)}) = \eta(1 - \eta)$ ,  $\mu(A_3^{(2)}) = \eta^2$ . Further on, a similar split of  $A_3^{(2)}$  into  $A_3^{(3)} = \{(x, y) : y = x^2 + \alpha^2 a - r\}$  and  $A_4^{(3)} = \{(x, y) : y = x^2 - r\}$  with  $\mu(A_3^{(3)}) = (1 - \eta)\eta^2$ ,  $\mu(A_4^{(3)}) = \eta^3$  follows. In this manner in the  $n$ th step of the above procedure we obtain a set  $\mathcal{A}_n$  of parabolic segments

$$\mathcal{A}_n = \bigcup_{i=1}^n A_i \cup A_{n+1}, \quad (5)$$

where  $A_i = \{(x, y) : y = x^2 + a\alpha^{i-1} - r\}$ ,  $\mu(A_i) = (1 - \eta)\eta^{i-1}$  and  $A_{n+1} = \{(x, y) : y = x^2 - r\}$ ,  $\mu(A_{n+1}) = \eta^n$  (cf. Fig. 1). The set  $\mathcal{A}_n$  is characterized by two parameters  $\alpha$  and  $\eta$ ; the additional parameter  $a$  just shifts the scale and is not important in further calculations.

To get the model of a real chaotic saddle we should, of course, put  $n \rightarrow \infty$ , but due to the limited precision in determining  $p - p_c$  in any measurement or simulation, taking

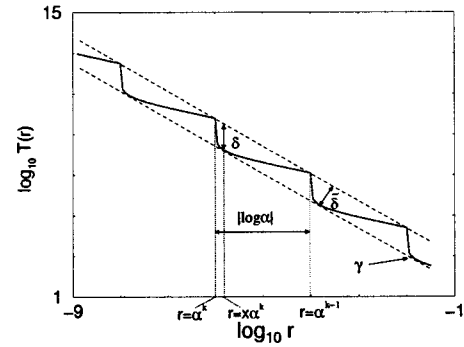


FIG. 2. Plot of the function  $T(r)$  for the model crisis at the parameter values  $a = 1$ ,  $\alpha = 0.01$ , and  $\eta = 0.01$ . The slope  $\gamma = 1.35$  [Eq. (8)]; amplitude of oscillations  $\delta = 1.32$  [Eq. (13)].

some large enough but finite  $n$  gives a sufficient approximation. Furthermore, in the real fractal set each segment of  $\mathcal{A}_n$  denoted by  $A_i$  has its own infinite fine structure, giving rise to a noninteger total fractal dimension. We ignore it in our model because it makes only a secondary contribution to the investigated oscillations. The parameter  $\alpha$  corresponds to the absolute value of the contracting eigenvalue  $\lambda_2$  of the orbit  $A(B)$  for a heteroclinic (homoclinic) crisis and determines the period of normal oscillations of  $T(r)$  in log-log scale.

### B. Amplitude of normal oscillations

Now consider the postcritical situation with  $r > 0$  (Fig. 1), when the attractor  $\mathcal{A}_n$  slides into the basin of attraction. Figure 2 shows the average transient lifetime  $T$  as a function of  $r$  obtained by taking the relation (4) as an equality. We can see the linear trend according to the power law (1), and additionally periodic oscillations imposed on it. The steps correspond to collisions of consecutive segments of  $\mathcal{A}_n$  with the half-plane  $y < 0$ , so their period equals  $|\log_{10} \alpha|$ . Our aim is to derive the amplitude  $\delta$  of the oscillations. In the first step, let us calculate the slope  $\gamma$ . To do this, consider one period of oscillations for  $r \in [\alpha^k, \alpha^{k-1}]$  (see Figs. 1 and 2). For small  $r$ , when  $\sqrt{r} \gg r$  is valid, the length of the parabola section  $y = x^2 + c - r$  that entered the basin of escape is approximately equal  $\sqrt{r - c}$  (for  $r > c$ ). Thus, the measure of the attractor in the basin of escape can be written as

$$\mu(r) = \eta^{k+1} \sqrt{r} + \eta^k (1 - \eta) \sqrt{r - \alpha^k}. \quad (6)$$

We assumed  $n = k + 1$  in Eq. (5), neglecting the further splitting of  $A_{k+2}$ . The slope is

$$\gamma = \frac{\log T(\alpha^k) - \log T(\alpha^{k-1})}{|\log \alpha|}. \quad (7)$$

Using Eqs. (4) and (6) and applying the approximation  $\sqrt{\alpha^{-1} - 1} \approx \alpha^{-1/2}$  for  $\alpha \ll 1$ , we get

$$\gamma = \frac{1}{2} + \frac{\log \eta}{\log \alpha}. \quad (8)$$

Comparing Eqs. (8) and (2) and remembering that  $\alpha = |\lambda_2|$ , we note that for a heteroclinic crisis  $\eta = 1/|\lambda_1|$ , so the parameter  $\eta$  has a simple interpretation in this case.

The quantity  $D = 1 + \log \eta / \log \alpha$  is the *pointwise dimension* of the attractor at the tangency point, it can be calculated directly from the definition [13] applied to  $\mathfrak{A}_n$  with  $n \rightarrow \infty$ . Equation (8) is in accordance with the relation  $\gamma = D - 1/2$ , which has been derived on the basis of the geometrical consideration in [14].

In order to calculate the amplitude of oscillations  $\delta$ , consider the derivative  $d(\log T(r))/d(\log r)$  [cf. Eqs. (4) and (6)]; it increases monotonically from  $-\infty$  at  $r = \alpha_+^k$  and tends to  $-1/2$  for  $r \rightarrow \alpha_-^k$  (see Fig. 2). At a value of  $r = x\alpha^k$ ,  $x \in (1, 1/\alpha)$  the function  $\log_{10} T(r)$  is tangent to its lower bounding line and the derivative

$$\left. \frac{d \log T(r)}{d \log r} \right|_{r=x\alpha^k} = -\gamma. \quad (9)$$

The amplitude of oscillations  $\delta$  can be calculated as the difference of the function  $\log_{10} T(r)$  and its upper bounding line at  $r = x\alpha^k$ :

$$\delta = \{ \log T(\alpha^k) - \gamma [ \log(x\alpha^k) - \log \alpha^k ] \} - \log T(x\alpha^k). \quad (10)$$

From the condition (9), using Eqs. (4), (6), and (8) we get, after some algebra,

$$x = \frac{2\kappa \frac{\gamma}{\gamma - \frac{1}{2}} - 1 - \sqrt{1 + 2\kappa \frac{\gamma}{\gamma - \frac{1}{2}}}}{2(\kappa - 1)}, \quad (11)$$

where

$$\kappa = (\alpha^{-(\gamma - 1/2)} - 1)^2. \quad (12)$$

Putting Eqs. (4) and (6) into Eq. (10) we get

$$\delta = \log \frac{\sqrt{x + \sqrt{\kappa(x-1)}}}{x^\gamma}, \quad (13)$$

with  $\kappa$  and  $x$  determined by Eqs. (12) and (11), respectively. The amplitude  $\delta$  may be considered as a function of two variables  $\alpha$  and  $\gamma$ . Taking into account that  $\alpha = |\lambda_2|$  and the exponent  $\gamma$  is given by Eq. (2) or Eq. (3),  $\delta$  (similarly to  $\gamma$ ) can be expressed in terms of the eigenvalues of the unstable periodic orbit involved in the crisis.

We can also define the width of the belt containing oscillations  $\tilde{\delta} = \delta / \sqrt{\gamma^2 + 1}$  (see Fig. 2) as the quantity describing the real visibility of the oscillations, unaffected by the slope  $\gamma$ . The width  $\tilde{\delta}$  is an increasing function of  $\gamma$  and a decreasing function of  $\alpha$ . The latter fact, as was mentioned, has already been noticed previously [8] for homoclinic crises.

### C. Numerical example: Boundary crisis in the Hénon map

We applied the formula (13) to boundary crises in the Hénon map,

$$\begin{aligned} x_{n+1} &= p - x_n^2 - Jy_n, \\ y_{n+1} &= x_n. \end{aligned} \quad (14)$$

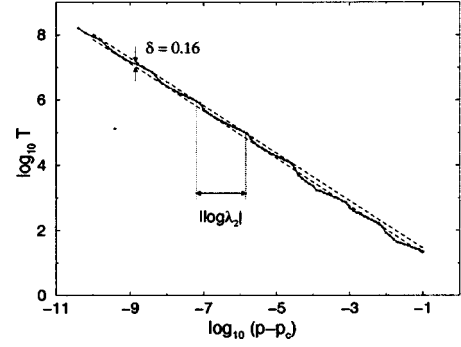


FIG. 3. Average transient length after the heteroclinic boundary crisis in the Hénon map for  $J = -0.1$  and  $p_c = 1.803\,239\,48\dots$ . The dashed lines indicate the amplitude of the attractor-induced oscillations calculated from our model, Eq. (13). The standard deviation is of the order of or below the size of the plotted points.

Consider, for example, the crisis at  $J_c = -0.1$  and  $p_c = 1.803\,239\,48\dots$ . For  $p < p_c$  there is a chaotic attractor that becomes a chaotic saddle after collision with an unstable fixed point at  $p = p_c$  (heteroclinic crisis). The basin of attraction is solid (no intertwined structure) near the boundary. For  $p \gtrsim p_c$  a typical orbit remains on the saddle for some time  $t$  and then rapidly diverges to infinity. Figure 3 shows the average length of the transients as a function of the distance from the crisis point. At every particular  $p$  the lengths of the transients were measured and averaged over a set of initial conditions from the basin of the precritical attractor. Oscillations superimposed on the linear trend with  $\gamma \approx 0.729$ , according to Eq. (2), can be seen. Their average period is approximately  $|\log_{10} \lambda_2| = 1.3$ . The dashed lines of the slope  $\gamma$  mark the amplitude of oscillations  $\delta \approx 0.16$  calculated from Eq. (13). One can see that it gives a good estimate for the size of the observed oscillations.

## III. CLOSER TO REALITY—BOTH KINDS OF OSCILLATIONS COMBINED

### A. Anomalous oscillations

As we have already mentioned in the introduction, another kind of oscillation imposed on the general trend described by Eq. (1), resulting from the intertwined structure of the precritical basins of attraction, may often be encountered. Let us briefly recall the model we developed in [9] in order to assess the maximal amplitude of the anomalous sections.

We defined the basin of escape (that was just the half-plane  $y < 0$  in the preceding section) in the vicinity of a collision point as a self-similar set  $\mathfrak{B}_n$  of stripes of the width  $\beta^i b_E$  accumulating at the geometric rate  $\beta$  to the line  $y = 0$ :

$$\begin{aligned} \mathfrak{B}_n &= \bigcup_{i=0}^n \{ \{x, y\} : y > -\beta^i b \wedge y < -\beta^i b + \beta^i b_E \} \\ &\cup \{x, y\} : y > -\beta^{n+1} b \wedge y < 0. \end{aligned} \quad (15)$$

As a model attractor, in turn, we took a single parabola  $y = x^2 - r$  (this would correspond to  $\mathfrak{A}_0$  from the previous model). The meaning of the quantities  $n$  and  $r$  is similar to that in the model from the preceding section.

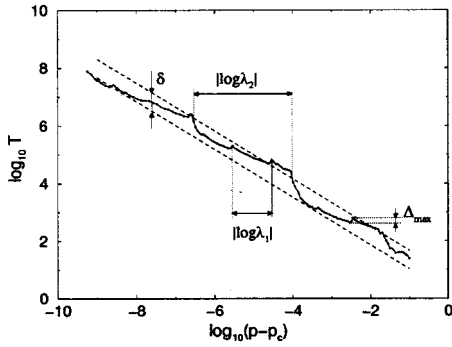


FIG. 4. Average transient length after the homoclinic boundary crisis in the Hénon map for  $J=0.3$  and  $p_c=2.124\,672\,43\dots$ . The dashed lines indicate the amplitude of the attractor-induced oscillations calculated from our model, Eq. (13). Tiny peaks of anomalous oscillations are visible.

Plotting  $\log T(r)$ , as in Fig. 2, we get saw-shaped oscillations of the period  $|\log \beta|$  determined by the scaling factor of the basin of escape, superimposed on a linear trend. Anomalous sections appear where  $T(r)$  is increasing. Carrying out a calculation similar to that for  $\gamma$  from the preceding section, we obtained an expression for the amplitude of the anomalous sections  $\Delta = \log T(r_2) - \log_{10} T(r_1)$ , where  $r_1$  and  $r_2$  denote, respectively, the beginning and end of the section (cf. Figs. 4 and 5):

$$\Delta = (1/\ln q) \sinh^{-1} \sqrt{S/\beta}, \quad (16)$$

where  $S = (b - \beta b - b_E)/b_E$  is the relative size of gaps in the basin and  $q$  is the base of the logarithms in the plot  $\log_q T$  vs  $\log_q r$  (in this paper we use  $q=10$ ).

We argued that the above formula gives the estimate for the *maximal* amplitude of anomalous oscillations that in real dynamical systems are only roughly regular. In fact, the attractor-induced oscillations are always present, but they are often dominated by the anomalous ones. Both kinds of oscillations can be distinguished on plots of  $T(p - p_c)$ , provided the amplitude of the anomalous ones is relatively small.

The parameter  $\beta$  in Eq. (15) corresponds to the inverse absolute value of the expanding eigenvalue  $\lambda_2$  of the medi-

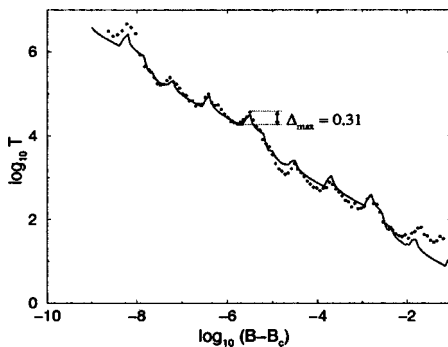


FIG. 5. Average time of residence on one of the precritical attractors after an attractor-merging crisis in the spin system for  $A_c=1$ ,  $\tau_c=2\pi$ ,  $\lambda_c=0.143\,700\,2\dots$ , and  $B_c=1$ . The solid line has been obtained by combining the self-similar attractor  $\mathfrak{A}_n$  and basin  $\mathfrak{B}_n$  models with the parameter values  $\alpha=0.002\,34$ ,  $\gamma=0.77$ ,  $\beta=0.124$ ,  $S=0.077$ , and  $b/a=3.83$ .

ating orbit  $B$ , whose stable manifold  $w_s^{(B)}$  is the basin boundary [10]. For homoclinic crises in strictly dissipative systems when  $|\lambda_1 \lambda_2| < 1$  the period of anomalous oscillations  $|\log \beta| = |\log \lambda_1|$  is always smaller than that of the normal oscillations  $|\log \alpha| = |\log \lambda_2|$ .

### B. Numerical example: Hénon map

As an example let us look at the average transient lifetimes after a homoclinic boundary crisis that occurs in the Hénon map (14) at  $J_c=0.3$  and  $p_c=2.124\,672\,450\dots$ . If we make the log-scale plot of  $T(p - p_c)$ , Fig. 4 (here  $T$  is again the length of chaotic transient before the escape to infinity, averaged over a set of initial conditions), measuring  $T$  with appropriate accuracy and marking subsequent points densely enough, we can see tiny anomalous peaks with average period  $0.97 \approx |\log \lambda_1|$ , where  $\lambda_1$  is the expanding eigenvalue of a period 3 orbit  $B$  mediating in a crisis. These oscillations are superimposed on the linear trend (1) and, dominating here, oscillations due to the ragged measure of the chaotic attractor. Again, the dashed lines show the amplitude of the normal oscillations calculated from Eq. (13).

Using the formula (16) we can calculate the maximal amplitude of anomalous oscillations  $\Delta=0.168$ . This value is very close to the maximal amplitude ( $\approx 0.16$ ) measured in Fig. 4. The parameter  $S \approx 0.0167$  has been determined from a few consecutive magnifications of the fractal basin boundary at the tangency point.

### C. Mixed case: Example of attractor merging crisis in a spin model

One can see that the models of the self-similar attractor and basin of escape in the vicinity of crisis tangency give a good assessment of the amplitude of attractor-induced oscillations and the maximal amplitude of anomalous oscillations, respectively, although a very simplified picture of much more complex real structures has been assumed. The self-similarity included in the models is, however, the main feature yielding the oscillations. To model the generic case when both kinds of oscillation appear together, we can combine both models observing  $T(r)$  when  $\mathfrak{A}_n$  penetrates  $\mathfrak{B}_n$ . One then obtains some irregular pattern of oscillations superimposed on the power law (1) (unless an exceptional set of parameters is used; e.g.,  $a=b$  and  $\alpha=\beta$ ). Nevertheless, the maximal amplitude of anomalous sections is determined by Eq. (16), and Eq. (13) gives a good approximation of the amplitude of normal oscillations  $\delta$ —provided they are not dominated by the anomalous ones.

To illustrate this and compare to a crisis in a real dynamical system, let us consider an attractor-merging crisis in a spin model describing the motion of a classical magnetic moment (spin)  $\mathbf{S}$ ,  $|\mathbf{S}|=S$  in the field of uniaxial anisotropy (easy/hard  $z$  axis) and transversal periodic impulse magnetic field  $\tilde{B}(t) = B \sum_{n=1}^{\infty} \delta(t - n\tau)$  along the  $x$  axis [15,16]. The system can be described by the Hamiltonian  $H = -A(S_z)^2 - \tilde{B}(t)S_x$ , where  $A$  is the anisotropy constant. The time evolution is determined by the Landau-Lifschitz equation with an added damping term:

$$\frac{d\mathbf{S}}{dt} = \mathbf{S} \times \mathbf{B}_{\text{eff}} - \frac{\lambda}{S} \mathbf{S} \times (\mathbf{S} \times \mathbf{B}_{\text{eff}}), \quad (17)$$

where  $\mathbf{B}_{\text{eff}} = -dH/d\mathbf{S}$  is the effective magnetic field and  $\lambda > 0$  is a damping parameter. Equation (17) can be transformed into a superposition of two two-dimensional maps [15,17] describing the time evolution between field impulses, and the effect of the impulse itself, respectively.

For  $A_c = 1$ ,  $\tau_c = 2\pi$ ,  $\lambda_c = 0.1437002\dots$ , and  $B \geq B_c = 1$ , we observe a crisis-induced chaos-chaos intermittency; i.e., random jumps between two symmetric precritical chaotic attractors. Figure 5 shows the average residence times  $T$  on one of the symmetric parts of the attractor as a function of  $B - B_c$  measured in a computer simulation together with the corresponding  $T(r)$  function ( $r = B - B_c$ ) obtained from the combination of the model attractor, Eq. (5), and basin of escape, Eq. (15). The ratio of the ‘‘initial size’’ parameters  $a/b$  that is now important was determined from the pictures of the attractor and basin tangencies at the crisis point, but it may also be treated as a fit parameter. The anomalous oscillations are clearly seen; their maximal observed amplitude again coincides with the value given by Eq. (16). One can also recognize a faint vestige of the attractor-induced oscillations, now veiled by the anomalous ones. It is notable that the model curve reproduces quite well the pattern yielded by the real dynamical system, despite the above mentioned simplifications. This proves the fact that the self-similar structure of the attractor and the basin included in the models is the basic feature underlying the emergence of oscillations. The whole finer fractal structure gives just secondary contributions. It also indicates the possibility of using the combined model to predict the behavior of the function  $T(p - p_c)$  for the  $p$  values very close to  $p_c$ , where the direct measurement is impossible because of very long transient times or the limited precision of determining  $p - p_c$ .

#### IV. SUMMARY AND CONCLUSIONS

We have investigated the deviations from the general power law governing the dependence of average transient times near crises. Two different kinds of oscillations have been distinguished: normal, caused by the self-similar (fractal) structure of the attractor; and anomalous, due to the self-similar intertwined structure of the precritical basins of attraction. The pure normal oscillations can be observed when the basins of attraction are solid, without intertwined structure. We showed, using a simple model of an attractor, that their amplitude is determined, similarly to the critical exponent  $\gamma$ , by the eigenvalues of the unstable periodic orbits involved in the crisis.

When basins are intertwined, both kinds of oscillations appear simultaneously, but the normal ones are visible only when the anomalous ones are relatively small. In a typical mixed case, a rather complicated pattern resulting from the interference of self-similar (fractal) structures of the attractor and basin is observed. The roughly periodic anomalous oscillations can, however, be noticed and their maximal amplitude can be calculated from a formula obtained on the basis of a simple model of a self-similar basin of attraction. Both models combined give a good approximation of the patterns produced by real dynamical systems and may be used to predict the behavior of  $T(p - p_c)$ ; e.g., in regions inaccessible to measurement.

The obtained results are applicable to a large class of two-dimensional systems undergoing different types of crises. The models can also be modified to get a still more detailed picture or to treat some special nongeneric cases.

#### ACKNOWLEDGMENTS

This work has been partially supported by the Polish Committee for Scientific Research (KBN), Grant No. 2P03B 031 14. A part of the calculations has been performed on the CRAY 6400 at the Warsaw University of Technology. We want to thank Wolfram Just for reviewing the manuscript and for his helpful remarks.

- 
- [1] C. Grebogi, E. Ott, and J. A. Yorke, Phys. Rev. Lett. **48**, 1507 (1982); Physica **7D**, 181 (1983).
  - [2] C. Grebogi, E. Ott, F. Romeiras, and J. A. Yorke, Phys. Rev. A **36**, 5365 (1987).
  - [3] C. Grebogi, E. Ott, and J. A. Yorke, Phys. Rev. Lett. **57**, 1284 (1986).
  - [4] J. C. Sommerer, W. L. Ditto, C. Grebogi, E. Ott, and M. L. Spano, Phys. Lett. A **153**, 105 (1991); I. M. Kyprianidis *et al.*, Phys. Rev. E **52**, 2268 (1995).
  - [5] M. Finardi *et al.*, Phys. Rev. Lett. **68**, 2989 (1992).
  - [6] R. W. Rollins and E. R. Hunt, Phys. Rev. A **29**, 3327 (1984).
  - [7] J. C. Sommerer and C. Grebogi, Int. J. Bifurcation Chaos Appl. Sci. Eng. **2**, 383 (1992).
  - [8] J. C. Sommerer, E. Ott, and C. Grebogi, Phys. Rev. A **43**, 1754 (1991).
  - [9] K. Kacperski and J. A. Hołyst, Phys. Lett. A **254**, 53 (1999).
  - [10] S. W. McDonald, C. Grebogi, E. Ott, and J. A. Yorke, Physica **17D**, 125 (1985).
  - [11] C. Grebogi, E. Ott, and J. A. Yorke, Phys. Rev. Lett. **56**, 1011 (1986); C. Grebogi, E. Kostelich, E. Ott, and J. A. Yorke, Physica **25D**, 347 (1987).
  - [12] C. L. Pando, G. Perez, and H. A. Cerdeira, Phys. Rev. E **48**, 196 (1993); E. Covas and R. Tavakol, *ibid.* **55**, 6641 (1997).
  - [13] C. Grebogi, E. Ott, and J. A. Yorke, Phys. Rev. A **37**, 1711 (1988).
  - [14] B. Pompe and R. W. Leven, Phys. Scr. **38**, 651 (1988); O. B. Christensen and T. Bohr, *ibid.* **38**, 641 (1988).
  - [15] J. A. Hołyst and A. Sukiennicki, Acta Phys. Pol. A **81**, 353 (1992); J. Magn. Magn. Mater. **104-107**, 2111 (1992).
  - [16] H. Frahm and H. J. Mikeska, Z. Phys. B **60**, 117 (1985); F. Haake, M. Kuś, and R. Scharf, *ibid.* **65**, 381 (1987).
  - [17] K. Kacperski and J. A. Hołyst, Phys. Rev. E **55**, 5044 (1997).